Chapter 5

The forward telescopes

5.1 System strategy

The measurement of the inelastic rate, which is necessary for the total cross-section determination, is performed by identifying all beam-beam events with detectors capable to trigger and to reconstruct the interaction vertex. Monte Carlo studies have shown that a good detector coverage in the forward region is necessary for a complete measurement of the inelastic rate. The main requirements of these detectors are:

- to provide a fully inclusive trigger for minimum bias and diffractive events, with minimal losses at a level of a few percent of the inelastic rate;
- to enable the reconstruction of the primary vertex of an event, in order to disentangle beam-beam events from the background via a partial event reconstruction (mainly the tracks coming from the primary vertex);
- a detector arrangement which is left-right symmetric with respect to the IP, in order to have a better control of the systematic uncertainties.

The requirements for such detectors are somewhat different from those for detectors that must guarantee detection and reconstruction of each particle in the event, which has influenced the choice of the technology for T1 and T2.

The TOTEM forward telescopes cover a rapidity range of about 4 units and are installed symmetrically in the forward regions of CMS (figure 1.1) on both sides ("arms") of the IP:

- T1 ($3.1 \leq |\eta| \leq 4.7$) is made of 5 planes per arm, each consisting of 6 trapezoidal Cathode Strip Chambers (CSC), and will be installed in the CMS End Caps between the vacuum chamber and the iron of the magnet, at a distance of 7.5 to 10.5 m from the IP.
- T2 ($5.3 \leq |\eta| \leq 6.5$) is made of 20 half circular sectors of GEM (Gas Electron Multiplier) detectors per arm and will be installed between the vacuum chamber and the inner shielding of the HF calorimeter at an average distance of 13.5 m from the IP.

In addition to the measurement of the total inelastic rate, T1 and T2 will be key detectors for the study of inelastic processes either by TOTEM or by the joint CMS/TOTEM experiments [2]. At low luminosities ($\mathscr{L} < 10^{31}\,\mathrm{cm}^{-2}\mathrm{s}^{-1}$):

- The integrated inclusive Single Diffractive (SD) and Double Pomeron Exchange (DPE) cross-sections can be measured, as well as their t and M_X dependence (where M_X is the mass of the diffractive system). SD and DPE events have a clean signature in TOTEM and can be triggered requiring at least one track in T1 or T2 in coincidence with the proton(s) detected in the Roman Pots.

- T1 and T2 contribute to the detection and measurement of the rapidity gaps in diffractive events, which may provide a complementary measurement of the fractional momentum loss of the surviving proton(s), as well as shed new light on the problem of the rapidity gap survival probability.

- The telescopes' coverage and granularity allow the measurement of the charged multiplicity in the forward region, providing important information for the cosmic ray physics community (mainly to tune their event generators). More details can be found in [26].

At higher luminosity, in the range $10^{31} < \mathscr{L} < 10^{33}\,\mathrm{cm}^{-2}\mathrm{s}^{-1}$, T2 can be used in the joint CMS/ TOTEM experiment for hard diffraction and forward physics studies. It can be used as a rapidity gap trigger in order to reduce QCD background in exclusive particle production in DPE events, as well as to help in very forward lepton identification in Drell-Yan pair production. The possibility of exploiting T2 track information in the study of rare processes such as single-diffractive proton dissociation into three very forward jets is still under investigation.

5.2 T1 telescope

5.2.1 Requirements and choice of detector technology

The T1 telescope, installed in two cone-shaped regions in the endcaps of CMS, detects charged particles in the pseudo-rapidity range $3.1 \leq |\eta| \leq 4.7$.

At $\mathscr{L} = 10^{28}\mathrm{cm}^{-2}\mathrm{s}^{-1}$ with a reduced number of bunches, the expected number of interactions per bunch crossing is expected to be 2.5×10^{-3} which translates to an inelastic interaction rate of about 1 kHz. The average number of charged particles per event in T1 is expected to be ~ 40.

The inelastic trigger plays an important role in the measurement of the total cross-section: one needs a minimum bias trigger with a very high and measured efficiency. Systematics in the measurement of the trigger efficiency will be studied using different trigger combinations and cross-checks of their stability during the measurement. The basic trigger elements (primitives) are arranged in a roughly pointing arrangement to perform, if necessary, a first level background suppression, and will be useful also to define the different sub triggers. To discriminate good beam-beam events from the background, which includes beam-gas interactions (pointing to different regions in z inside the beam pipe) and other machine backgrounds such as the muon halo (approximately parallel to the beam), TOTEM needs to reconstruct only a number of tracks sufficient to reconstruct the position of the interaction vertex and check that it is compatible with the interaction point.

A detector with a well-known technology to meet these general requirements is the multi-wire proportional chamber with segmented cathode read-out: the Cathode Strip Chamber (CSC).

2008 JINST 3 S08007

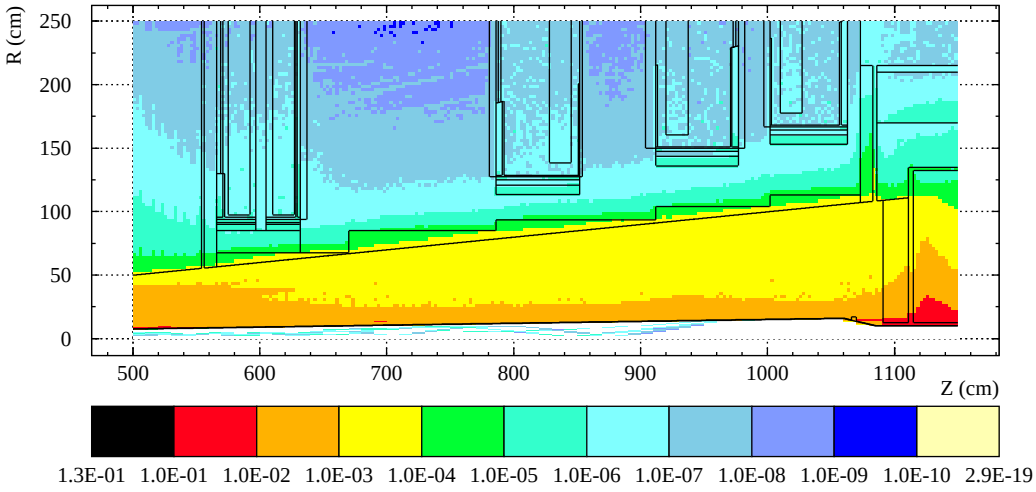

Figure 5.1: Expected accumulated dose, in Gy, from a simulation for 1 s at $10^{34}\,\mathrm{cm}^{-2}\mathrm{s}^{-1}$ luminosity, in the region occupied by T1.

These detectors, in which a single gas gap with segmented cathode planes allows a two-dimensional measurement of the particle position, are well understood (see for example [27]). Gas detectors of this kind are slow, but the response time for a CSC with a 10.0 mm gas gap is still compatible with the expected hit rates for TOTEM. Moreover, TOTEM's CSCs can be built in shapes suitable to cover the required area of the T1 telescope. They have small material densities which is important because they are positioned in front of forward calorimeters.

Another delicate parameter to consider is the behaviour in a high-radiation environment. Detailed simulations [28] estimate the flux of charged and neutral particles and the accumulated dose in the T1 region (figure 5.1).

The ageing properties of the TOTEM CSCs have been tested at the Gamma Irradiation Facility at CERN: two chambers have been irradiated, integrating a total charge on the anode wires of 0.065 C/cm, without showing any loss of performance, in agreement with tests performed by CMS [29]. This accumulated dose is equivalent to about 5 years of running at luminosities of $10^{30}\mathrm{cm}^{-2}\mathrm{s}^{-1}$. In the outer region of T1, where the cathode read-out electronics will be installed, the expected dose is lower by about two orders of magnitude.

5.2.2 Detector and telescope design

5.2.2.1 Detector geometry

The two *arms* of the T1 telescope, one on either side of the IP5, fit in the space between two conical surfaces, the beam pipe and the inner envelope of the flux return yoke of the CMS end-cap, at a distance between 7.5 m and 10.5 m from the interaction point. The telescopes will be the last to be inserted when closing and the first to be removed when opening the CMS detector.

Each telescope consists of five planes of CSCs, equally spaced in z, numbered as 1 to 5 from the closest (smallest) to the farthest (largest) from the interaction point. The vacuum chamber is

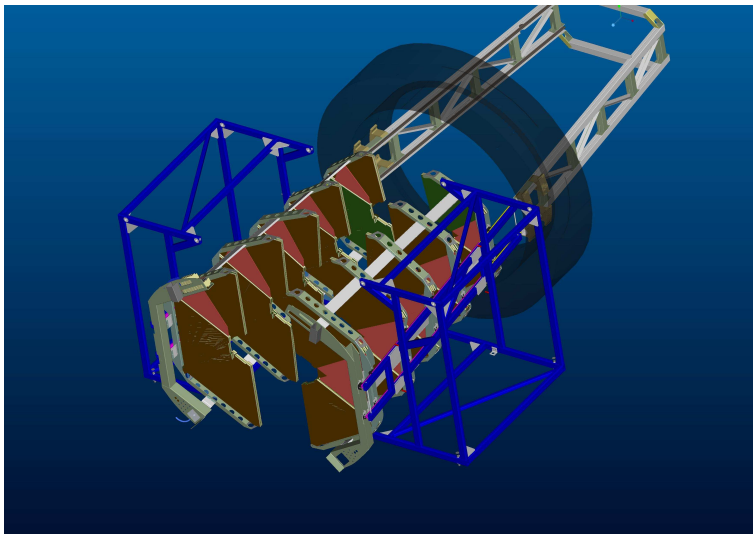

Figure 5.2: The two halves of one T1 telescope arm before insertion in CMS.

in place and aligned when the installation of T1 takes place: for this reason each telescope arm is built in two vertically divided halves (*half arms*) as depicted in figure 5.2.

A detector plane is composed of six CSC wire chambers covering roughly a region of 60° in ϕ and, as mentioned above, is split in two halves and mounted on different supports. Overlap is provided between adjacent detectors (also for the ones on different supports) to cover with continuous efficiency the approximately circular region of each telescope plane. In addition, the detector sextants in each plane are slightly rotated with respect to each other by angles varying from $-6°$ to $+6°$ in steps of 3°, the "reference" orientation being that of layer 5. This arrangement is useful for pattern recognition and helps to reduce the localised concentration of material in front of the CMS HF (Hadronic Forward) Calorimeter.

The conical volume reserved for the telescope contains also the mechanical support structure for installation inside the CMS end cap, which implies the construction of CSC detectors of 10 different dimensions (2 different types in each plane identified by the codes *n*G, *n*P). Figure 5.3 shows the layout of the 30 detectors of one arm.

5.2.2.2 Description of the T1 detectors

CSCs have been studied in detail in RD5 [27], and CSCs of very large dimensions have been built for ATLAS [30], CMS [31] and LHCb [32]. The TOTEM CSCs use basically the same technology developed for the other larger experiments, which we want to acknowledge here, tailoring specific parameters to the TOTEM requirements.

An exploded view of the different components making up a chamber assembly is shown in figure 5.4.

Two stiff panels of trapezoidal shape determine the flat surfaces of the cathode planes. A thin continuous frame is inserted between the two panels to keep with a good precision the two cathode planes parallel with a gap of 10.0 mm. The frame also has the function of defining a tight volume in which high purity gas will be flushed with a slight overpressure of a few g/cm^2.

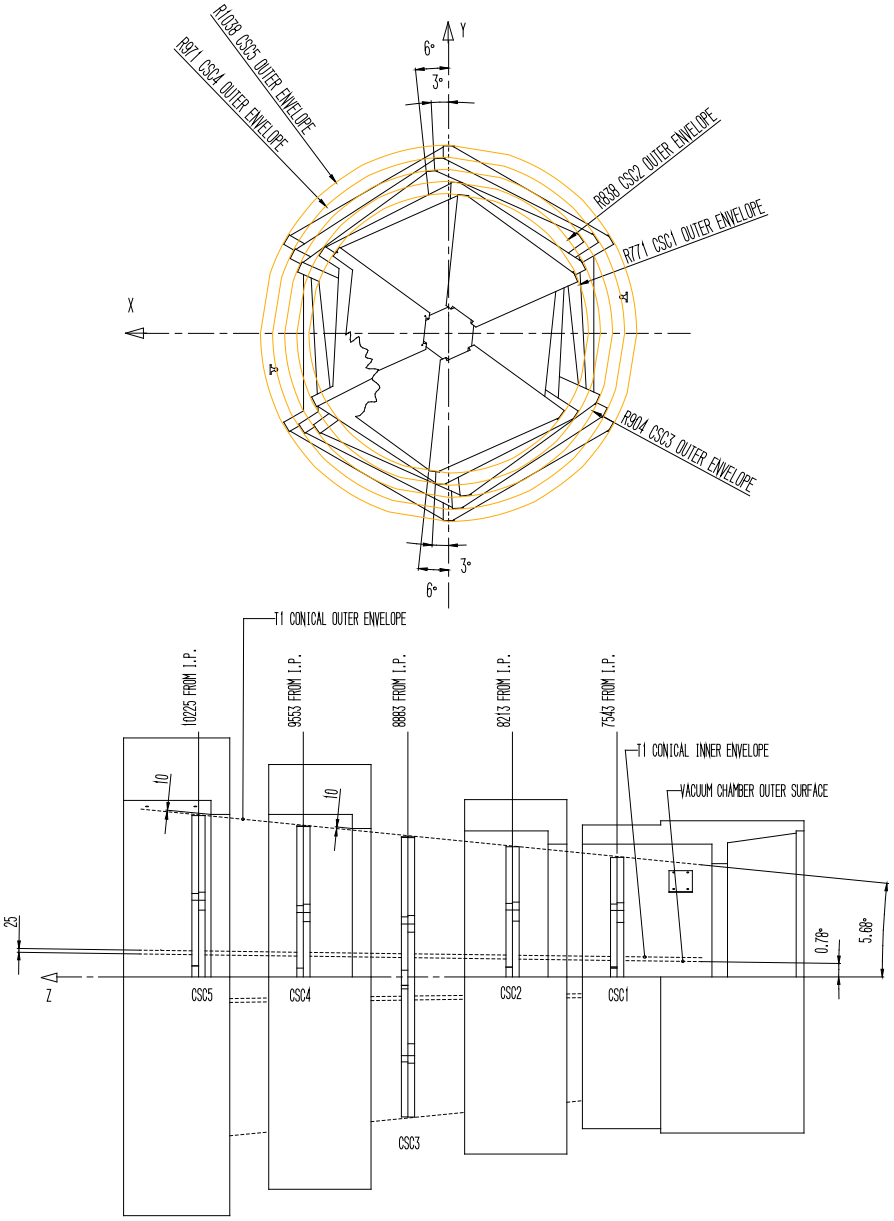

Figure 5.3: Layout of one T1 detector arm. The front view (left) shows the small rotations of the different planes.

The cathode panels are composite structures, sandwich panels of standard glass-epoxy laminates with a core of honeycomb, and provide the necessary stiffness. A study and tests were performed to optimise the thickness of both skins and of the core in the sandwich panel, in order to meet the stability requirements under load and minimise the material of the detector. The two panels are made with a 15 mm thick Nomex hexagonal honeycomb, enclosed between two 0.8 mm thick "skins" of fiberglass/epoxy laminate. Both skins are covered by a 35 μm thick copper layer. Cathode strips are etched and gold-plated with standard PCB technology on one of the two skins of a panel before its manufacture. The correct width of the gas gap is ensured by a G-10 frame glued

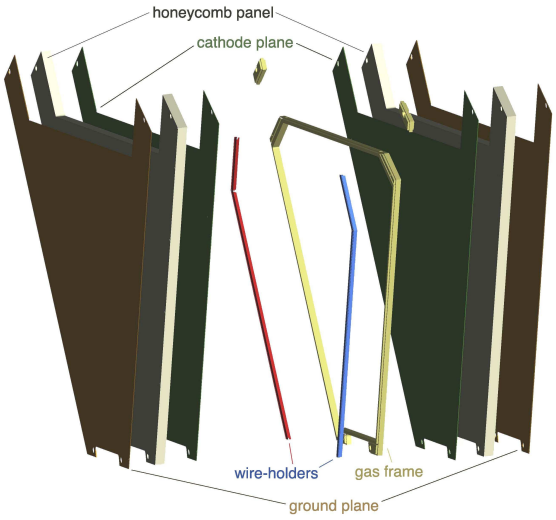

Figure 5.4: Exploded view of a TOTEM CSC detector.

to one of the two panels ("gas frame"). Besides acting as spacer, the frame guarantees gas tightness to the detector and gas distribution. The gas input and output lines enter the detector in the large side of the trapezoid and continue through a narrow duct machined through the full length of the sides: uniform gas distribution to the sensitive volume of the detector is achieved on each side via six equally spaced holes of 1.0 mm diameter.

The anode of the detector is composed of gold-plated (gold content of 6–8%) tungsten wires with 30 μm diameter, produced by Luma Metall;[1] the wires are strung parallel to the base of the trapezoid with a tension of 0.7 N at a pitch of 3.0 mm. The support for the wires ("wire holder" in figure 5.5) is provided by two printed circuit bars precisely machined to a thickness of 5.0 mm glued on the wire panel along the oblique sides of the detector and inside the gas volume. The wires are soldered and glued to pads on top of the bars; the pads are in turn electrically connected to tracks on the external region of the cathode plane. The first and the last anode wire, close to the inner and the outer edge of the detector, are field-shaping electrodes and have a larger diameter (100 μm). High voltage is applied on one side; on the opposite side the front-end card is directly soldered to pads connected to each single anode wire.

The cathode electrodes are parallel strips obtained as gold-plated tracks oriented at $\pm 60^\circ$ with respect to the direction of the wires and have 5.0 mm pitch (4.5 mm width and 0.5 mm separation). Each strip is connected to high-density connectors mounted outside the gas volume as shown in figure 5.5.

The orientations of the cathode strips and of the anode wires allow for three measurements in the plane of the position of the avalanche thus providing three measured coordinates for each particle track, which significantly helps to reduce the number of fake hits from random combinations ("ghosts").

The geometrical parameters of all 10 types of chambers are summarised in table 5.1; the numbers of anode and cathode read-out channels are listed in table 5.2.

[1] LUMA METALL AB, S-39127 Kalmar Sweden.

2008 JINST 3 S08007

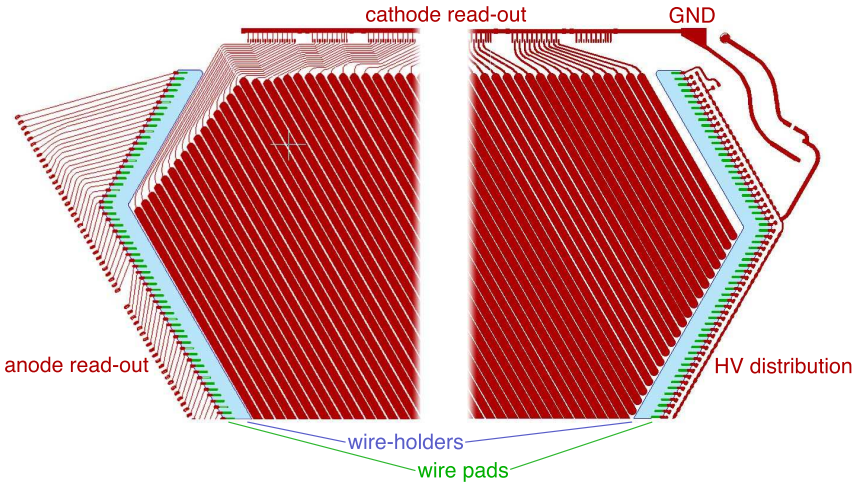

Figure 5.5: Cathode strips and wire-holder printed circuit boards.

Table 5.1: CSC geometrical parameters.

detector type	1G	1P	2G	2P	3G	3P	4G	4P	5G	5P
major base width [mm]	766	641	833	717	894	751	967	840	1016	957
minor base width [mm]	233	233	244	244	255	255	267	267	260	290
height [mm]	498	385	546	453	591	477	642	543	681	615
gas gap	10 mm									
anode wire spacing	3 mm									
anode wire diameter	30 μm									
cathode strip pitch	5 mm									
cathode strip width	4.5 mm									

Table 5.2: T1 read-out channels.

chamber type	1G	1P	2G	2P	3G	3P	4G	4P	5G	5P
wires per anode plane	165	127	181	150	196	158	213	180	226	204
strips per cathode plane	118	97	129	108	137	114	150	127	164	150
total anode channels	11124									
total cathode channels	15936									

5.2.2.3 T1 detector production

Immediately after assembly, the T1 CSC are submitted to a set of acceptance tests. The gas gain uniformity is measured by displacing a point-like ^{90}Sr radioactive source on the surface of a CSC operated at a high voltage of 3.6 kV, flushed with an Ar/CO_2 (50/50) mixture and measuring the current drawn by the power supply (figure 5.6).

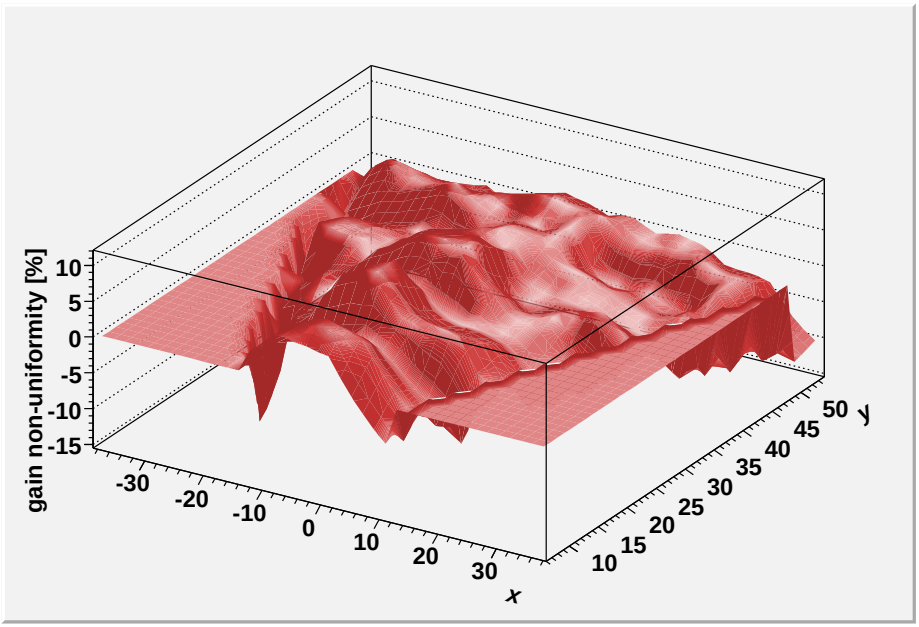

Figure 5.6: Gas gain uniformity deviations over a TOTEM CSC.

Figure 5.7: Completed CSC chambers for T1 in a test area at CERN.

After arriving at CERN, the detectors are submitted to further tests; figure 5.7 shows completed CSC chambers in the assembly laboratory.

The detectors that compose a half-plane are then secured to an aluminium frame with an overlap of the sensitive areas between them of few centimeters. Each of the five detector planes of one half telescope, plus a sixth frame that supports patch panels for the connections of the "services" (readout lines, trigger lines, high voltage, low voltage and gas and cooling lines), is fixed

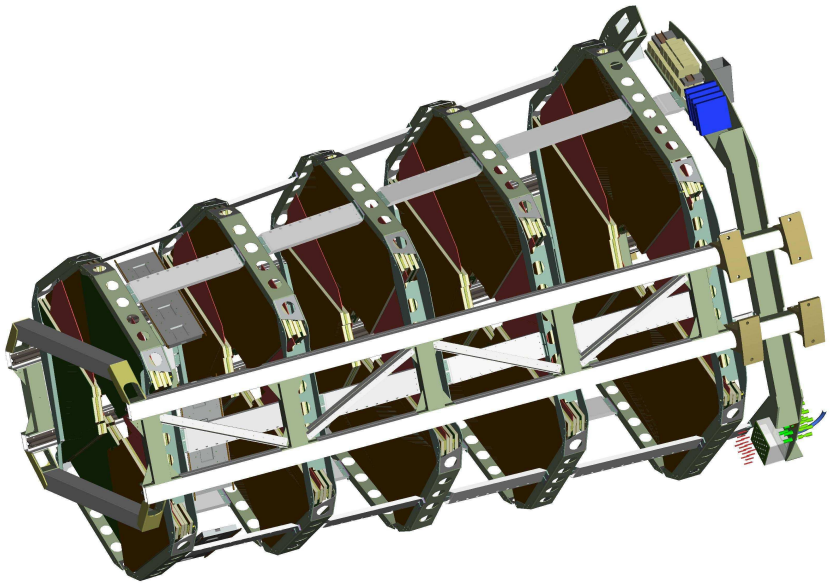

Figure 5.8: T1 assembly (one arm) with support structure. Some of the spacers between the detector planes and one support bar for the cathode read-out electronics are visible. On the right-hand side, the service support frame and the fixation plates securing the whole assembly to the internal surface of the CMS flux return yoke can be seen.

separately to the rails. The relative positions of the planes are defined by a series of appropriately positioned aluminium spacers. One telescope arm (two halves) in its final position on the truss is shown in figure 5.8.

5.2.2.4 Support structure and installation in CMS

The installation of the T1 telescope inside the CMS end-cap is delicate due to the tight geometrical constraints. Firstly, the zone is only accessible through the front circular opening and the installation can only be made when the end-caps are in place. Secondly, the beam pipe is also in place and the detector must be "closed" very carefully around it, avoiding contact with the two vertical rods supporting the pipe. Thirdly, the path of several CMS alignment laser beams traverse the volume of T1 and must be kept free.

Each of the two telescopes is therefore vertically divided in two halves, with independent support structures and services.

Two steel trusses are bolted to the third sector (YE3) of the CMS end cap, the same that supports the vacuum pipe, thus minimising any possible movement of T1 relative to the vacuum pipe as a result of the end cap deformation when the magnet is switched on. To guarantee the minimum acceptable deformation under load and at the same time minimise the cross-section of the structure, the trusses are joined together at the other end by two transverse bars. At installation T1 slides in position on rails mounted on each truss.

2008 JINST 3 S08007

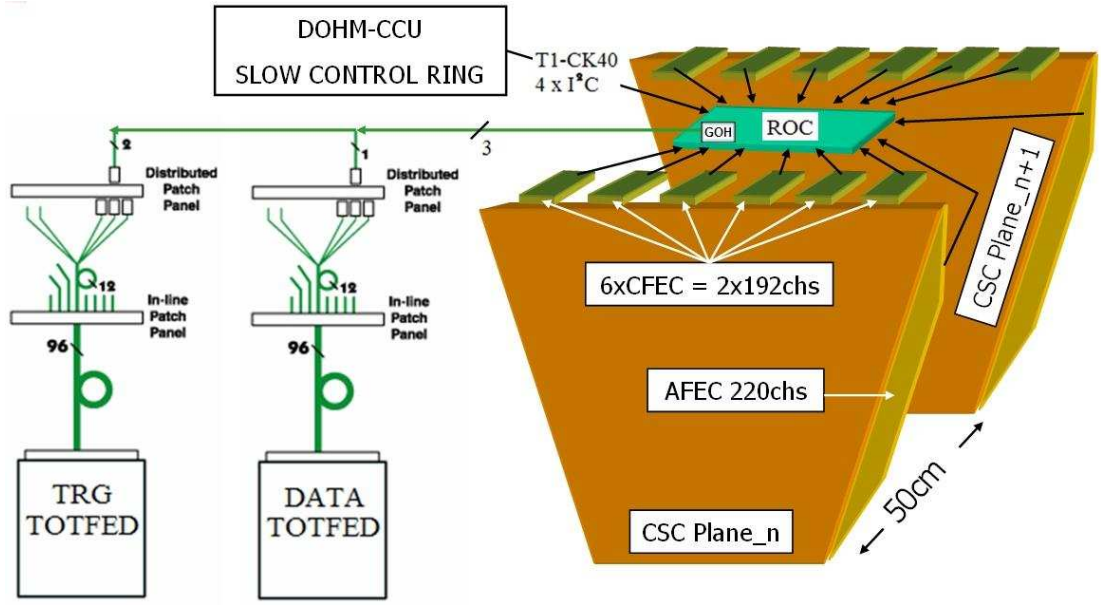

Figure 5.9: Overview of the T1 electronics system.

The half telescope is assembled and prepared for installation inside a specific structure with two rails similar to the truss ones. The half planes of T1 are mounted on this temporary structure, equipped with read out electronics, connected and tested. The structure also serves as support for the service racks of T1. For installation the structure is positioned on top of the HF calorimeter, the rails on the end cap and on the structure are aligned and the two telescope halves are slid into position inside the CMS end-cap. After this operation the CMS HF calorimeter can be raised to its final position, with the T1 external support structure still on its top.

5.2.3 T1 electronics system

The CSC anode and cathode signals are collected by custom-designed Anode Front-End Cards (AFEC) and Cathode Front-End Cards (CFEC), and conditioned by dedicated VLSI devices [33]. The serial digital data stream and the trigger signals coming out from the AFEC and CFEC are collected by the custom-designed Read-Out Card (ROC [33]) where they are serialised and optically transmitted to the DAQ system through a dedicated CMS Gigabit Optical Hybrid (GOH) [34]. The configuration and monitoring of the system is performed by the I^2C standard protocol distributed through the optical CMS Slow Control Ring SCR (DOHM [35] + CCUM [36]).

The T1 electronic front-end system globally involves 60 AFEC, 252 CFEC, 36 ROC, 96 GOH, 4 DOHM, 36 CCUM, while the T1 DAQ structure is based on a TOTEM custom board that can perform data (data FED) and trigger (trigger FED) signal analysis (section 7.2.2). An overview of the system is shown in figure 5.9.

5.2.3.1 AFEC

The AFEC is the board that collects and groups the anode wires of the CSC detector. Due to the conic structure of the telescope, ten different types of AFECs have been adapted to the chambers, for a total of 60 boards installed. The AFECs are soldered directly on the edges of the chambers, and the dimensions vary between 60 cm and 100 cm. The AFEC contains for every channel a double-stage high-pass filter isolating the high voltage on the wire from the readout, and adapting impedance and signal shape. The readout of up to 256 wires per chamber is carried out by two VFAT chips (section 7.1), each mounted on a VFAT hybrid (section 5.3.4) connected to the AFEC through a compact 130 pin connector.

Trigger information, permitting both individual TOTEM and CMS-integrated runs, is generated on the VFAT by grouping anode wire signals into 16 groups to form primitive hits for road reconstruction.

The connection of the AFEC to the ROC board, that represents the superior level of the DAQ chain, is realised by two high-density halogen free 50-wire cables.

5.2.3.2 CFEC

The CFEC is the board that collects and groups the cathode strip signals of the CSC detector. Each board processes 128 input signals with a passive network and delivers the outputs to a VFAT chip on a VFAT hybrid connected to the CFEC through a compact 130 pin connector. Due to the different sizes of the detectors, for each layer of the telescope a different number of CFEC boards are needed.

In order to improve the position resolution, a second version of the board has been designed and tested. In the new board the analog signal processing is performed by the BUCKEYE and LCT-COMP devices [37], developed for the CMS Muon project. The BUCKEYE chip includes a 5th order preamplifier, shaper and tail cancellation stages, while the LCT-COMP performs the discrimination of the BUCKEYE analog outputs. Each comparator output is serially coded on three bits (TRIADE) that contain the information about the side (right or left) of the strip where the charge is distributed.

The serial decoding of the discriminator outputs and the management of the slow-control features of the CFEC, like threshold settings, channel masking and calibration, are accomplished by an ACTEL Antifuse FPGA (A54SX32A)[2] device.

5.2.3.3 ROC

The ROC board represents the data, trigger and low voltage junction point of the T1 detector front-end boards and performs a similar function for the CSCs as the motherboard for the RPs. Each card is able to acquire data and trigger bits from two CSC detectors.

The board receives data from 16 VFAT hybrids hosted on the AFEC and CFEC cards, for a total of 2048 CSC signals.

The serial data stream received from the front-end is converted from LVDS to CMOS level, connected to the GOH mezzanine and optically transmitted to the DAQ system through the custom data FED board in the counting-room (section 7.2.2 and Ref. [38]).

[2] SX-A Family FPGAs, Actel Corp., February 2007.

Each detector has allocated up to 8 front-end connections, divided in two for the anodes and six for the cathodes. Only the AFECs produce trigger information. For each detector a total of 16 trigger bits are generated and transmitted to the TOTEM trigger system (trigger FED board) via a dedicated GOH optical link. The trigger information can also be merged with the data using a spare Gigabit Optical Link data channel and a special VFAT trigger hybrid.

For slow control, the CMS tracker and ECAL token ring system was adopted: similar to the RP system, a CCUM mezzanine mounted on the ROC forms a node in the slow control token ring. This system contains a skip fault architecture for additional redundancy based on doubling signal paths and bypassing of interconnection lines between CCUMs. Each CCUM controls the reset signal, three 8-bit general-purpose I/O ports and up to 16 I^2C serial line connections.

The 40 MHz master clock and the LHC fast commands are extracted in the ROC also from the token ring, and regenerated by CMS PLL devices (PLL25 [39] and QPLL). The distribution of the clock and the LHC fast commands to the front-end boards is implemented adopting a tree structure in order to minimise the skew and the delay time between different front-end receiver circuits.

In order to avoid missing data in case of failure of the master VFAT that enables the GOH serial data transmission, redundancy logic has been foreseen in the design of the ROC. The swapping of the master VFAT can be done via the general purpose I/O bits available through the SCR. As for the data, also the trigger bit transmission is modifiable changing the functionality of the logic with the SCR I/O connections.

A spy test port is foreseen on the ROC board, all the front-end connections are routed to dedicated connectors in order to plug a piggy-back mezzanine where a dedicated Xilinx FPGA (XC3S1500FG456)[3] and USB 2.0 logic can emulate the DAQ system chain.

5.2.3.4 High and low voltage supplies

The high and low voltage distribution for the CSC detectors is organised per half telescope arm (15 detectors). The high voltage system is based on the 24 channel A1550P board [40] (5 kV, 1 mA) and the CAEN SY1527 controller [41] placed in the counting-room.

The low voltage has to be applied locally, and thus the Wiener Marathon system [42] was chosen for its robustness against radiation and magnetic fields. One crate with 12 channels (2-8 V, 55 A) provides digital and analog power separately for half a telescope arm.

5.3 T2 telescope

5.3.1 Requirements and Choice of Detector Technology

The T2 telescopes, located at ± 13.5 m on both sides of IP5 (figure 1.1), detect charged particles in the pseudorapidity range of $5.3 \leq |\eta| \leq 6.5$. Generic requirements for the T2 (like for T1) include a fully inclusive trigger for diffractive events, hit pattern reconstruction for vertex finding to be used in discriminating against possible beam-gas background and for left-right symmetric alignment of telescopes for better control of the systematic effects.

The T2 telescope has been designed for good coverage of forward physics processes with varying beam conditions both at low luminosities (total cross-section and soft diffractive scattering)

[3] Xilinx Inc., *Spartan-3 FPGA family — v. DS099*, 25 May 2007.

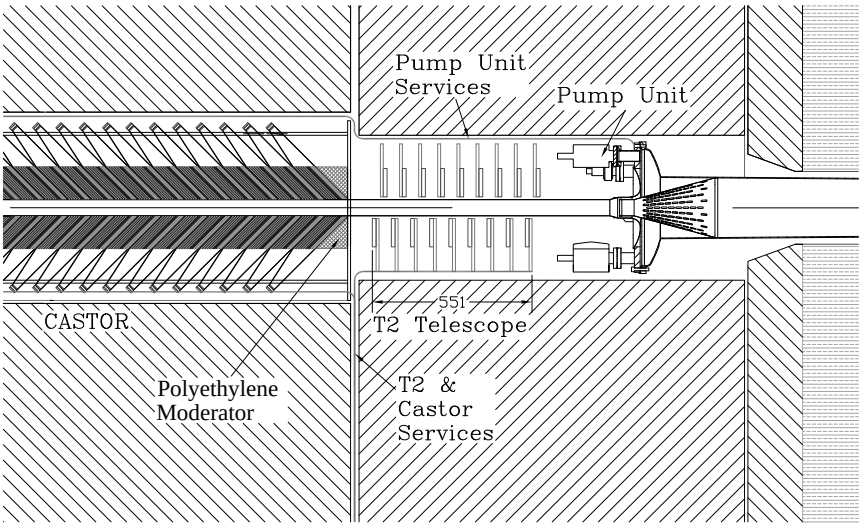

Figure 5.10: The location of the TOTEM T2 telescope within the shielding of CMS.

and at moderate luminosities (semi-hard diffractive scattering, low-x physics). Moreover, the T2 telescope is expected to operate up to luminosities of the order of $10^{33}\,\mathrm{cm}^{-2}\mathrm{s}^{-1}$ [1] where hard diffraction, heavy particle searches and physics beyond the standard model could be probed.

Due to the shape of the LHC vacuum chamber at the T2 location, an increased rate of particle-wall interactions is expected and had to be carefully considered. As a result, a compact detector array with a resolution in polar angle, $\Delta\theta/\theta$, matching the corresponding T1 resolution was adopted as a design criterium.

The gaseous electron multipliers (GEM) were selected for detectors of the T2 telescope thanks to their high rate capability, good spatial resolution, robust mechanical structure and excellent ageing characteristics. Invented a decade ago by Fabio Sauli [43] and studied by numerous research groups in experimental high energy physics, the GEM technology may be considered as a mature technology for the LHC environment. Excellent results of the COMPASS experiment [44], obtained during running periods extending over several years in high-rate environment, support also the choice of the GEM technology. Consequently, the COMPASS GEM design was adopted as a guideline for the GEMs of the TOTEM T2 telescope.

5.3.2 Detector Layout

5.3.2.1 The Telescope

The T2 telescopes are installed in the forward shielding of CMS between the vacuum chamber and the inner shielding of the HF calorimeter. There is a vacuum pump unit in front of T2 and the CMS CASTOR calorimeters behind it (figure 5.10). To reduce the neutron flux at T2 and HF, an additional polyethylene moderator will be installed between T2 and CASTOR. According the CMS simulations performed with the FLUKA Monte-Carlo package, the expected fluence of charged particles is around $10^6\,\mathrm{cm}^{-2}\mathrm{s}^{-1}$ with the moderator installed [1].

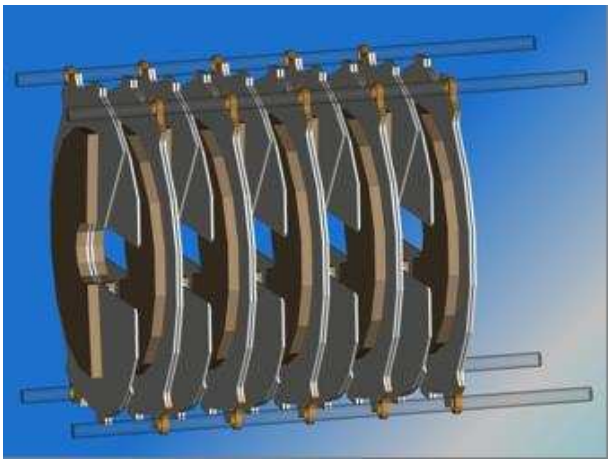

Figure 5.11: A CAD drawing depicting the arrangement of the 20 consecutive half-planes of Gaseous Electron Multiplier (GEM) detectors into one of the two T2 telescopes. In each detector layer, two GEM half-planes are slid together for maximal azimuthal angle coverage. With the ten double detector layers both high efficiency for detecting the primary tracks from the interaction point and efficient rejection of interactions with the LHC vacuum chamber is achieved.

In each T2 arm, 20 semi-circular GEM planes – with overlapping regions – are interleaved on both sides of the beam vacuum chamber to form ten detector planes of full azimuthal coverage (figure 5.11). The GEMs are installed as pairs with a back-to-back configuration. This arrangement of active detector planes allows both track coordinates and local trigger – based on hit multiplicities and track routes pointing to the interaction region – to be obtained. The material budget of T2 telescopes is minimised by using low-Z construction materials and honeycomb structures in manufacturing the GEM support mechanics.

5.3.2.2 T2 GEM Detectors

The shape of the GEM detector used in T2 telescope is semi-circular with an active area covering an azimuthal angle of 192° and extending from 43 mm up to 144 mm in radius from the beam axis (figure 5.12).

The design of the T2 GEM detector is based on utilisation of the standard GEM foils manufactured by the CERN-TS-DEM workshop. The foil consists of 50 μm polyimide foil (Apical) with 5 μm copper cladding on both sides. Due to the bidirectional wet etching process used by the workshop the shapes of the holes are double conical. The diameters of the holes in the middle of the foil and on the surface are 65 and 80 μm, respectively.

Three GEM foils are used as a cascade in one detector (figure 5.13) to reduce the discharge probability below 10^{-12} [45]. For the same reason the voltage divider supplying the voltages for the foils is designed such that the potential difference is gradually decreasing from the uppermost foil to the lowest one (nearest to the readout board). Moreover, the high voltage side of each foil is divided into four concentric segments for limiting the energy available for sparks (figure 5.14).

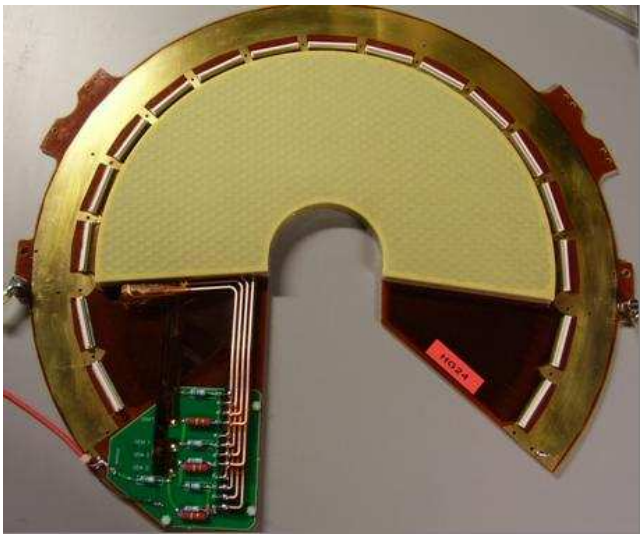

Figure 5.12: The TOTEM T2 GEM detector without front-end electronics and cooling pipes.

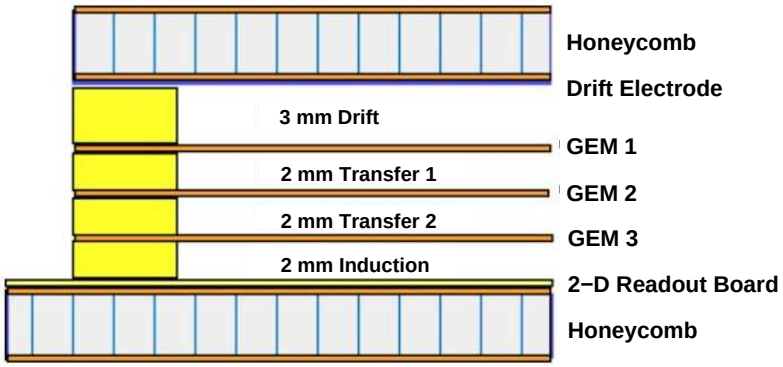

Figure 5.13: A side view of the T2 GEM detector structure: Three Gaseous Electron Multiplier (GEM) amplification stages are realised by three perforated and Cu-clad polyimide foils supported by honeycomb plates. A 3 mm drift space is followed by two 2 mm deep charge transfer regions (Transfer 1 and Transfer 2) and a 2 mm charge induction space. The large signal charges are collected, in two dimensions, by a read-out board underneath of the induction layer. The lightweight construction and support materials are chosen for low-Z material budget and mechanical robustness.

The segments are biassed separately through high voltage resistors, enabling switching off the innermost segment if required. The ground sides of the foils are continuous.

At the design value of the operating voltage, the gas amplification over all the three foils will be roughly 8000, a value selected by the COMPASS experiment too. Consequently, the average amplification over a single foil is typically 20. The thickness of the drift space is 3 mm, whereas the transfer 1 and 2 and the induction gaps are all 2 mm (see figure 5.13). The corresponding electric fields over the gaps are approximately 2.4 kV/cm and 3.6 kV/cm, respectively.

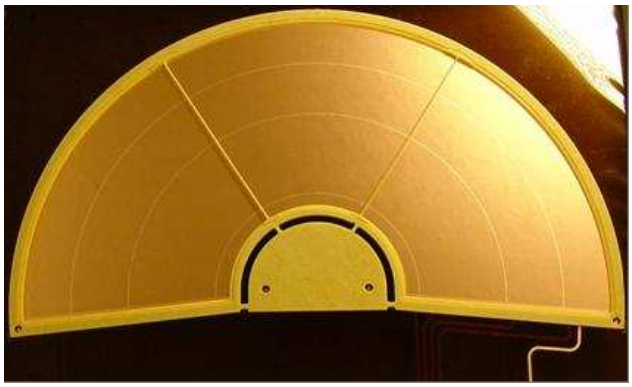

Figure 5.14: The T2 GEM foil glued to the support frame. The division of the electrode into four ring segments to minimise the energy available for discharges is visible.

The GEM foils are stretched and glued over supporting frames, which are manufactured by Computer Numerical Control (CNC) machining from fiberglass reinforced epoxy plates (Permaglas) with thicknesses of 2 mm. Two additional supporting spacers of thickness 0.5 mm are designed in the middle of the frames (see figure 5.14). Their position is slightly asymmetric to minimise dead areas. The drift frame is similar, except that the thickness is 3 mm and that no thin spacers in the middle of the frame are used.

An outgassing analysis of the frame material revealed emission of several organic compounds. Most of them were solvent-like remnants from the manufacturing process. One of these was toluene, which is known to cause ageing in ordinary wire chambers [46]. To remove the solvents from the material, all the frames were baked in a vacuum oven for several hours at a temperature of 80°C.

A polyimide foil with a copper cladding (5 μm) on a single side with thickness of 50 μm is used as a drift electrode which is glued to the front plate. The front and back plates are honeycomb structures, in which a honeycomb sheet of thickness 3 mm (Nomex) is sandwiched between two thin FR4 sheets of thickness 125 μm and enclosed inside a supporting frame made of the same material as the frames of the foils. The readout board is glued to the back plate.

A printed circuit board covered by polyimide foil with a pattern of strips and pads is used as a two-dimensional readout board. The rather complicated structure is manufactured partly by a commercial company and partly by a CERN workshop (TS-DEM group). The readout board contains 2×256 concentric strips for the radial coordinates and a matrix of 1560 pads for azimuthal coordinates and for the T2 local trigger (figure 5.15).

The strips lie on top of the pads and are isolated from the pads by a thin layer of polyimide, which is removed between the strips by wet etching (figure 5.16). The width and spacing of the strips are 80 and 400 μm respectively. To reduce the occupancy, the strips are divided into two parts, each covering 96° in azimuthal angle. The readout of the strips is located on both ends of the chamber.

The pads are divided into 65 radial sectors each containing 24 pads with sizes ranging from $2 \times 2\,\mathrm{mm}^2$ close to the vacuum chamber wall to $7 \times 7\,\mathrm{mm}^2$ at the outer edge of the semi-circular planes. The charge collected by the pads is read, with help of vias and strips on the backside of the board, at the outer edge of the readout board.

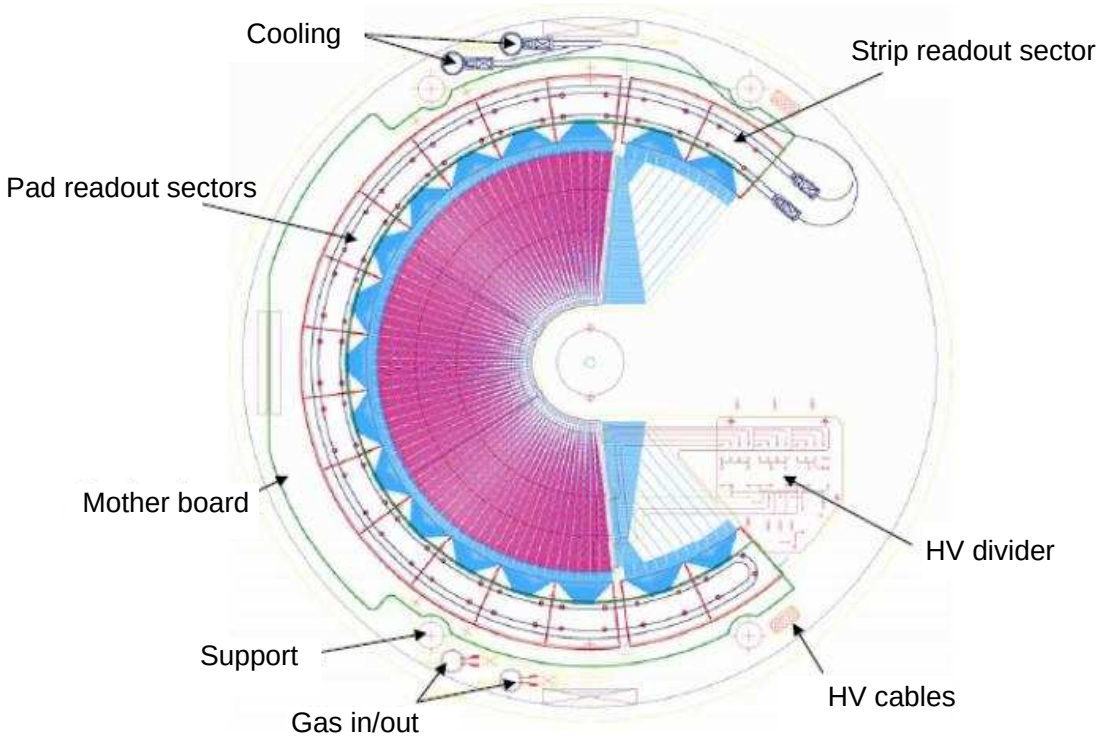

Figure 5.15: The design drawing of the TOTEM T2 GEM detector.

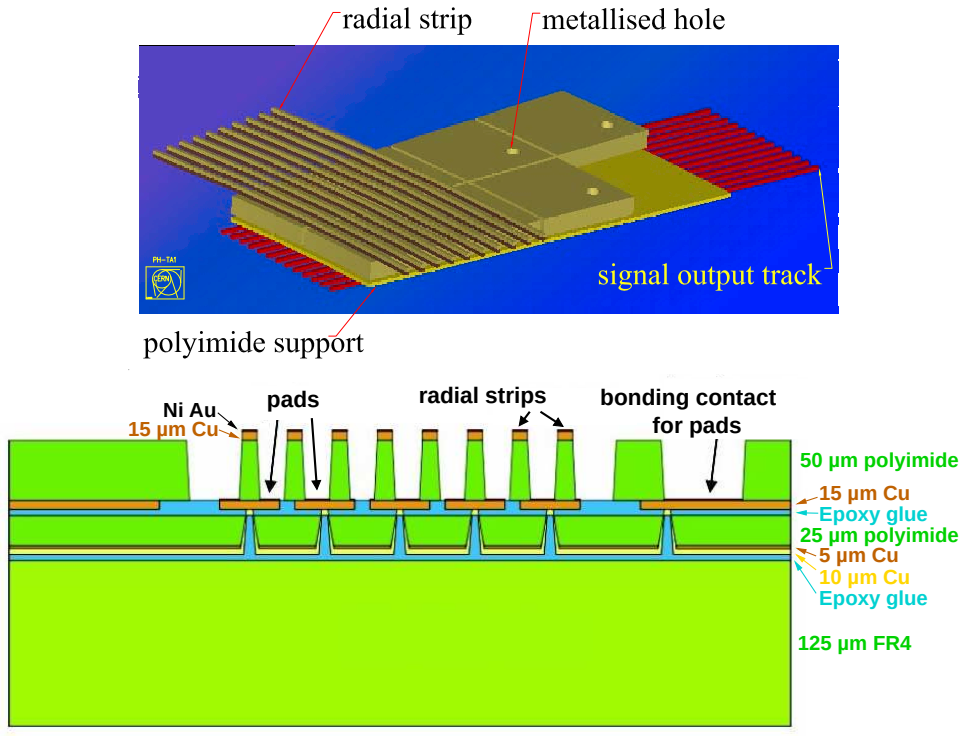

Figure 5.16: Detailed views of the strip/pad structure of the T2 GEM readout. Top: 3-dimensional view, bottom: cross-section.

Unlike in the COMPASS experiment, the readout electronics are connected to the readout board by connectors. No wire bonding on the readout board is required. SMD-connectors of 130 pins with 0.5 mm pitch are soldered directly on the board. Four connectors are required for the strip readout (128 strips per connector) and 13 for the pad readout. The pad connectors are hence used to read five sectors of 24 pads (120 pads), the other pins in the connectors are grounded.

The gas connectors are also installed on the readout board. The fill gas of the GEM (Ar/CO_2 70/30 mixture) is supplied through channels engraved in the fiberglass frame beneath the polyimide foil. The frames of the GEM foils contain also holes in two corners for a uniform distribution of the gas to the drift, transfer and induction gaps.

5.3.3 Detector Manufacture

The production of the required 50 individual GEM detectors (2×20 detector planes for the left and right T2 telescopes, 10 in reserve) was initiated in summer 2006 in Helsinki. Due to the harsh operating environment in the forward region, special care has been taken in devising efficient quality control processes both for the GEM components and their overall performance criteria.

The GEMs are almost exclusively manufactured in clean rooms of the Detector Laboratory where a dedicated assembly line for the large GEM detectors was set up. Although the production process is mostly based on manual assembly phases, some of the quality-control related tasks are made automatic. These include leakage current measurements of the GEM foils, optical inspection of the foils and search for broken or short-circuited strips/pads on the readout board.

An automatic leakage current measurement system for the GEM foils was devised and consists of a programmable electrometer, a special arrangement for electric contacts and a LabView based software package. The GEM foils are considered acceptable when the leakage current stays over half an hour below 0.5 nA at a test voltage of 500 V over the foil in dry atmosphere.

In addition to the leakage current measurement, the quality control of the GEM foils contains visual inspection of the foils and optical scanning of the whole foil surfaces. The aim of the scanning is to record the known defects of the foils for later use. A commercial flatbed scanner and an external background lighting setup are combined for automatic GEM foil scanning. The foils are scanned from each side with a resolution of 2400 dpi. Background light is utilised for spotting the holes in which the polyimide layer was incompletely etched or when the hole was entirely absent on the other side of the foil. In addition to finding defects on the surface of the foil, the system is also used for measuring the variation of hole sizes across the foil area.

Broken strips and short circuits between strips and pads may cause data corruption and additional noise in GEMs. These defects are easily seen in capacitance values of the strips and the pads. Due to the large number of channels (1560 pads and 512 strips), a special automated capacitance measurement system for the strips and pads of the GEM readout boards was developed. The system consists of a computer controlled x-y table, a programmable LCR-meter and a custom-made test board. The pad geometry, with pads growing larger when moving from inside out in radial direction from the beam vacuum chamber wall, is clearly seen in the resulting graphs. The measured variation of strip capacitances is relatively small.

In the finishing stage of the manufacturing process the basic characteristics of the GEMs filled with a gas mixture of Ar/CO_2 (70/30) are measured in the laboratory with the help of standard ^{55}Fe

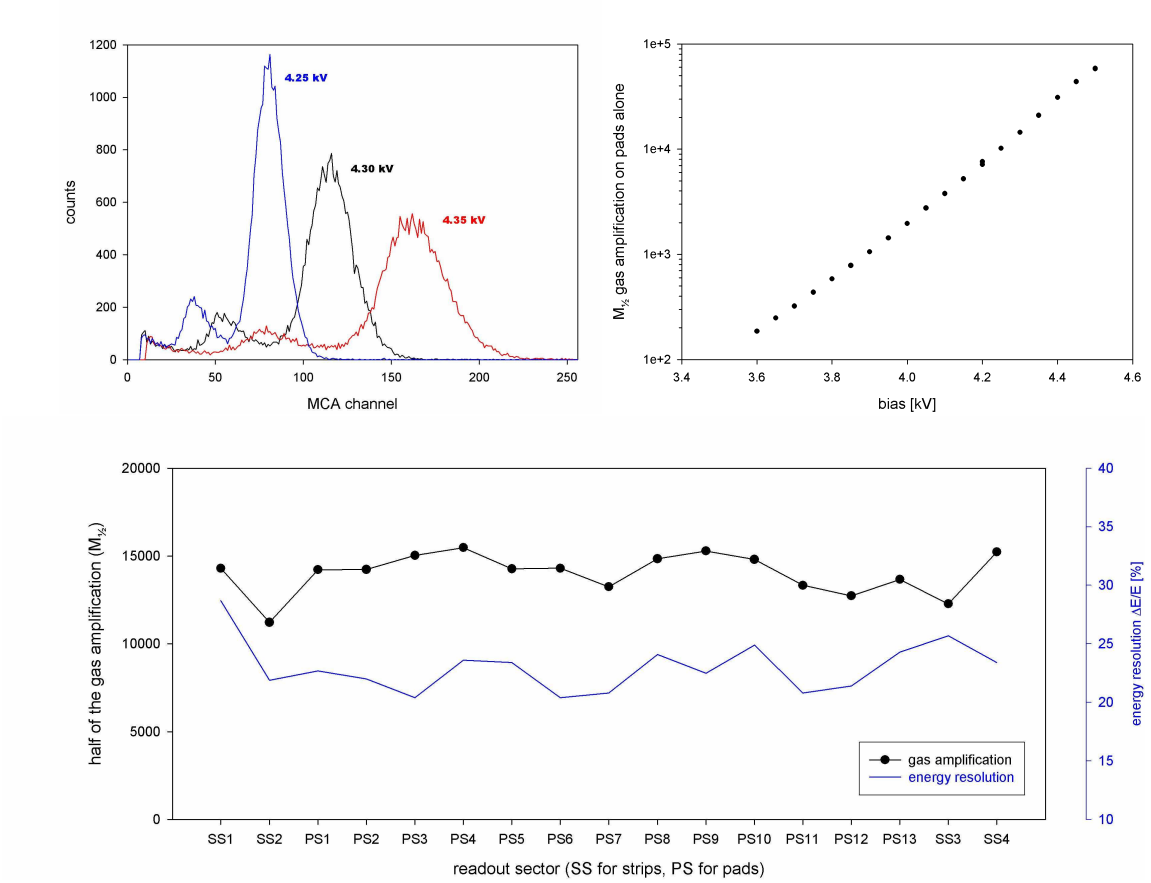

Figure 5.17: Examples of operational tests of the T2 GEMs with gas mixture Ar/CO_2 (70/30) done after the detector assembly: a) ^{55}Fe X-ray spectra at different bias voltages, b) a gas amplification vs. bias voltage, c) variation of the gas gain and the energy resolution over the readout sectors.

X-ray sources (5.9 keV). These consist of gas amplification and energy resolution measurement at different bias voltages and in different readout sectors (figure 5.17). All the GEMs are tested with a gas amplification up to 10^5, which corresponds to a gain one order of magnitude higher than the design value. Moreover, the characteristics of the GEMS and their readout electronics are tested in several beam tests during the years 2006-2007.

5.3.4 On-detector electronics

The T2 detector consists of 40 GEM detectors arranged in 4 quarters of 10 detectors. Each detector is read out by 17 VFATs 13 for the pads (120 pads per VFAT) and 4 for the strips (128 strips per VFAT). Each VFAT is mounted on its own VFAT hybrid (figure 5.18). All 17 VFAT hybrids of one GEM detector are mounted on a "horseshoe card" named after its physical shape (figure 5.19) The horseshoe cards of the 10 detectors of one T2 telescope half arm are connected to the so-called "11th card" which provides the interface to the outside world. A schematic view of the entire system is shown in Figure 5.20.

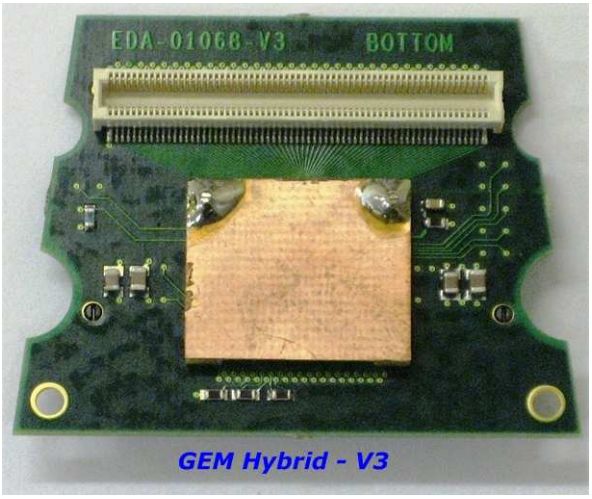

Figure 5.18: The TOTEM gas detector hybrid carrying one VFAT readout chip (under the cover).

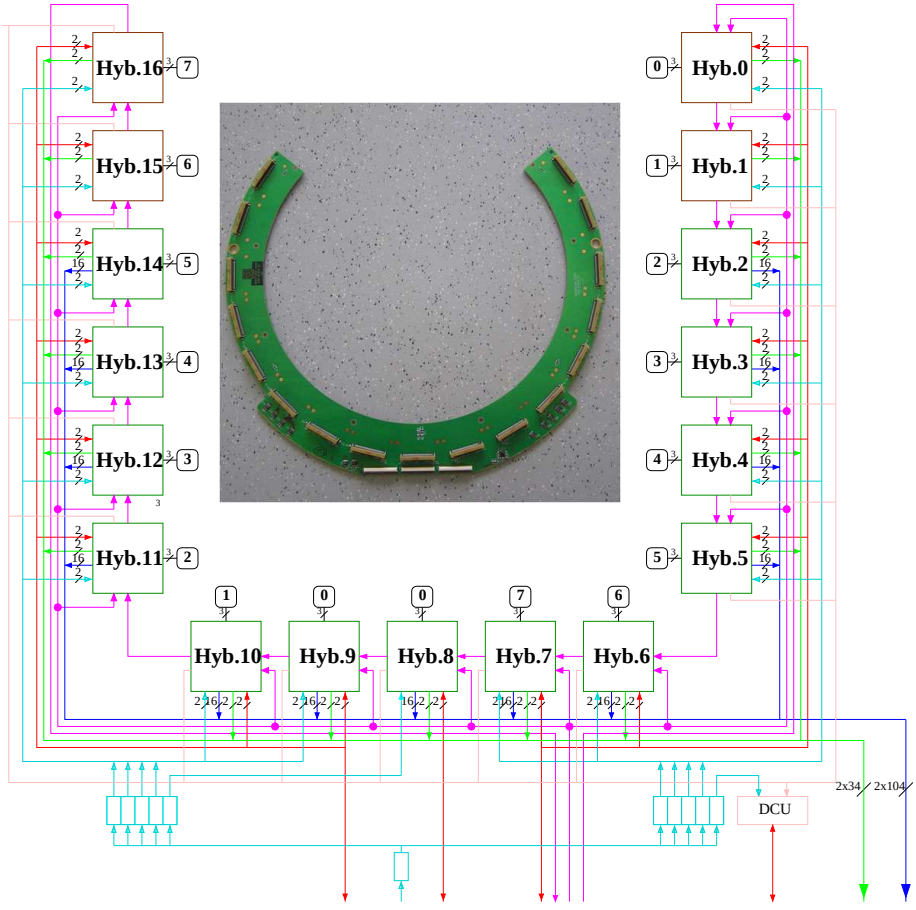

Figure 5.19: Architecture of the Horse-Shoe card (red for I^2C lines, cyan for clock and trigger lines and LVDS buffers, pink for DCU and monitoring lines, blue for trigger hybrid outputs, green for data and data valid hybrid outputs, magenta for scan test lines, dark green for pad VFAT hybrids, dark brown for strip VFAT hybrids).

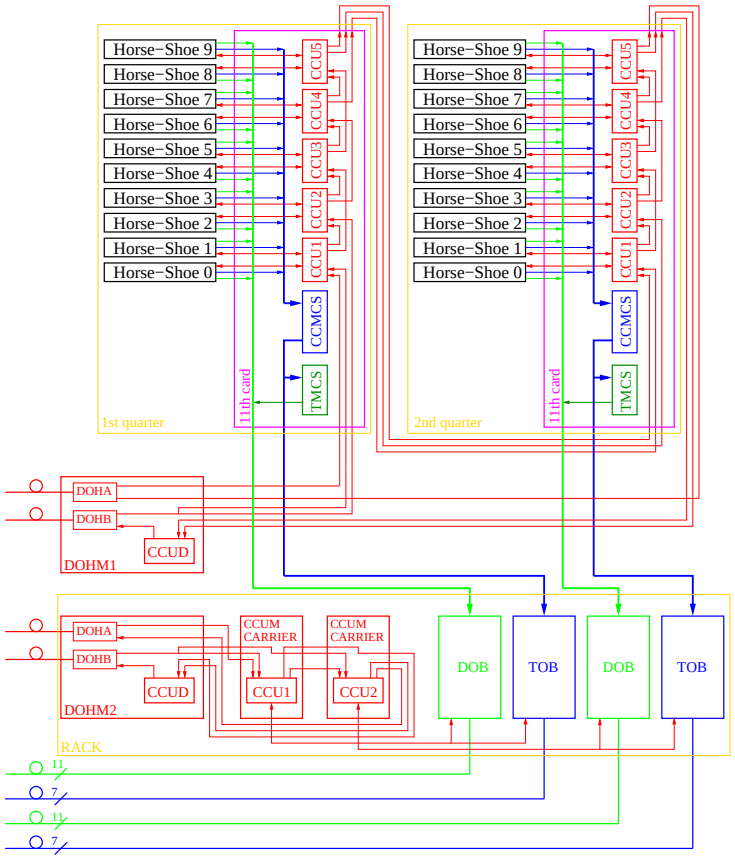

Figure 5.20: Architecture of the readout electronics of half of the detector (black for Horse-Shoe cards, magenta for 11th cards, red for CCUMs, DOHMs and control, clock and trigger lines, blue for trigger hybrid outputs, CCMCs and Trigger Opto-Boards, green for data outputs and Data Opto-Boards, dark green for TMCs and TMC outputs to Data Opto-Boards.)

The VFAT hybrids are linked to their horseshoe card by a 50-pin connector transmitting:

- precision data and trigger data from the VFATs to the horseshoe card, and
- clock, trigger and control signals, HV and LV power from the horseshoe card to the VFAT hybrids.

5.3.4.1 Data Path

The precision data (green lines in figure 5.20) and the tracking data (blue lines) originating from all hybrids of a T2 half arm (or quarter of the full telescope) are transmitted via the 10 horseshoe cards to the 11th card (magenta boxes in the figure) which performs coincidence analysis on the grouped trigger data coming from the VFAT fast-or logic. For the latter purpose, the 11th card houses 13 mezzanine cards equipped with a coincidence chip (CCMCs, blue boxes).

Both full-precision data as well as results of the trigger coincidence logic are sent from the 11th card to Opto-Boards equipped with GOHs (Gigabit Optical Hybrids) for optical transmission

to the counting-room. The extreme radiation levels in the T2 station preclude the use of optohybrids on the 11th card, which therefore had to be placed in a rack on the GEM platform just outside the shielding of the detector. Data transmission to the optohybrids is carried out electrically using LVDS signals over about 6 metres.

Since one GOH can handle up to 16 data lines, the $10 \times 17 = 170$ precision data lines from a T2 half arm are regrouped in the 11th card and sent to 11 GOHs mounted on one Opto-Board ("Data Opto-Board", green boxes "DOB" in the figure).

The $13 \times 8 = 104$ trigger outputs of the CCMCs are also regrouped and sent to 7 GOHs mounted on a second Opto-Board ("Trigger Opto-Board", blue boxes "TOB" in the figure).

In order to include trigger information into the data stream, a second branch of the 104 trigger signal lines is regrouped into two sets of 64 and 40 signals respectively and sent to 2 Trigger Mezzanine Cards (TMCs, dark green boxes in the figure) equipped with a VFAT chip. Each TMC generates a data stream containing trigger information that is sent to the Data Opto-Board together with the output data from the VFAT hybrids.

For the whole T2 system 8 optoboards are foreseen, 4 on either side, 2 for each half arm, one for tracking data and one for trigger data.

5.3.4.2 Controls

A Detector Control Unit (DCU) on the horseshoe card monitors temperature, analog and digital power supply voltages, and the output voltages and currents generated in the DAC integrated in the VFAT chips. The DCUs are controlled via I^2C links by Communication and Control Units (CCUs), each of them mounted on a CCU mezzanine card (CCUMs) on the 11th card. With 1 CCU per 2 horseshoe cards, each 11th card is equipped with 5 CCUs. The 2×5 CCUs on the two 11th cards of each T2 arm communicate with the control token ring via 1 Digital Opto Hybrid Module (DOHM). See also section 7.2.1.

The controls for the Opto-Boards are generated by two additional CCUMs mounted on CCUM carriers in the rack on the GEM platform outside the detector shielding. These CCUMs are connected to a second DOHM for communication with the control token ring.

The clock signals and trigger commands for the Horseshoe cards, the TMCs, the CCMCs and the Opto-Boards are distributed by the CCUMs after extraction from the control token ring.

5.3.4.3 Power Supplies

Two 11th cards and the 20 connected horseshoe cards are powered by a 12-channel Wiener Power Supply. Eight channels are used for analogue and digital power supply voltages of odd and even Horse-Shoe cards connected to the two 11th cards. Two other channels are used to power the first DOHM and the CCUMs in the 11th cards and the second DOHM, the CCUM in the CCUM carriers in the rack and the Opto-Boards respectively. Two channels are used as spares.

5.3.5 Detector Performance

Some of the TOTEM GEM detectors underwent several tests in a laboratory setup as well as in an SPS testbeam. The aim of these tests was to verify the performance and quality of the GEM detectors, the optimisation of the noise level measured with the TOTEM VFAT readout chip.

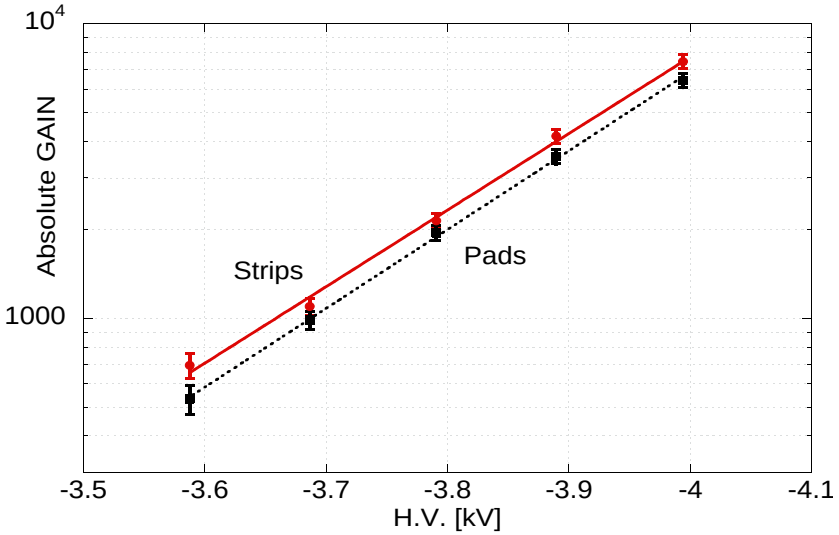

Figure 5.21: Absolute Gain calibration as a function of the applied High Voltage for strips (solid) and pads (dashed). This calibration curve was obtained with a Cu X-ray tube source, by measuring the X-ray interaction rate in the gas and the current collected by strips and pads.

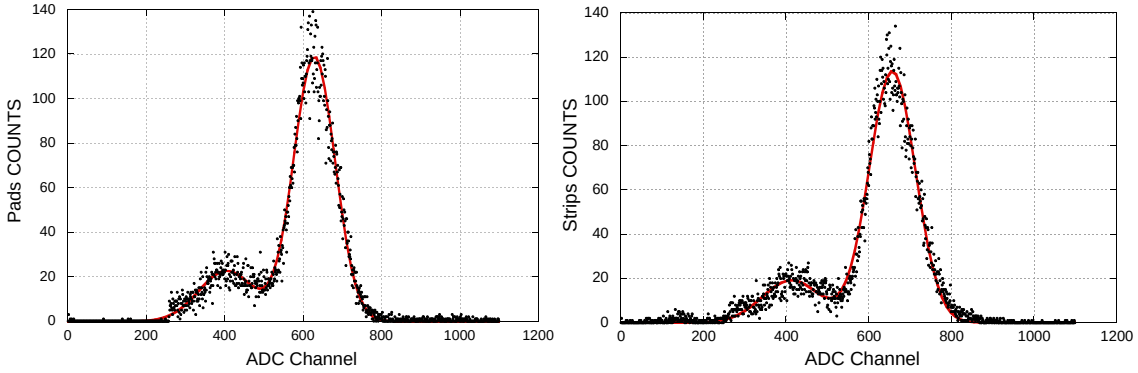

Figure 5.22: Cu X-ray spectrum as measured with a group of 48 pads (left) and with a group of 16 strips (right) on a GEM with a high voltage of -4 kV.

The absolute gain calibration curve for strips and pads irradiated by a Cu X-ray tube is shown in figure 5.21 as a function of the High Voltage applied. The comparison of the results of this test for different positions on the sensitive area of each detector and between different chambers, is in agreement with the expectations.

Figure 5.22 shows typical spectra obtained with a Cu X-ray tube, from which we can extract information about energy resolution (figure 5.23, left) and charge sharing between strips and pads (figure 5.23, right). These spectra were obtained with a 142IH ORTEC charge preamplifier and an ORTEC 450 research amplifier while the detector was powered with a HV of -4 kV.

Tests of GEMs equipped with the final TOTEM readout chip VFAT have been done to study the combined performance. Figure 5.24 shows the noise level for some strips (left-hand and mid-

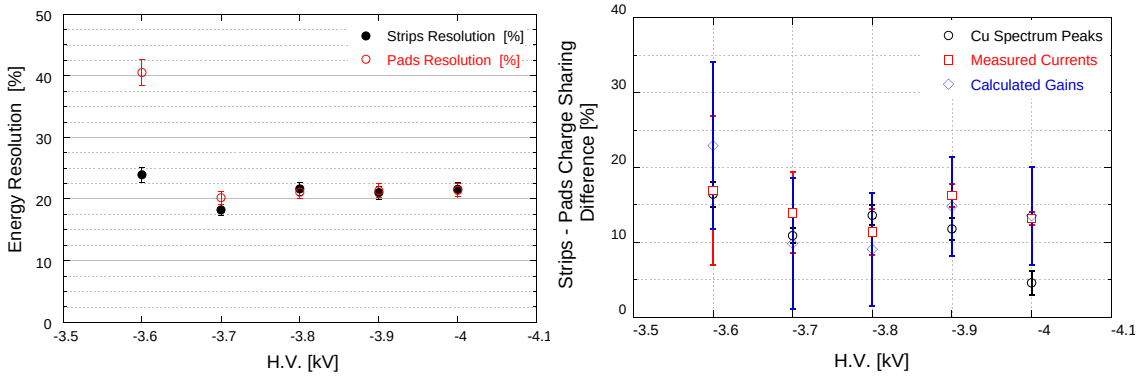

Figure 5.23: Left: energy resolution for strips and pads measured on the Cu Kα (and Kβ) emission peaks as a function of the applied HV. Right: charge sharing between strips and pads (open circles), as obtained by the relative difference between the positions of the Cu $K\alpha$ peak of strips and pads obtained from spectra analogous to the ones in figure 5.22. Also shown are the relative differences between the currents collected from strips and pads (open squares), and between the gains (open diamonds).

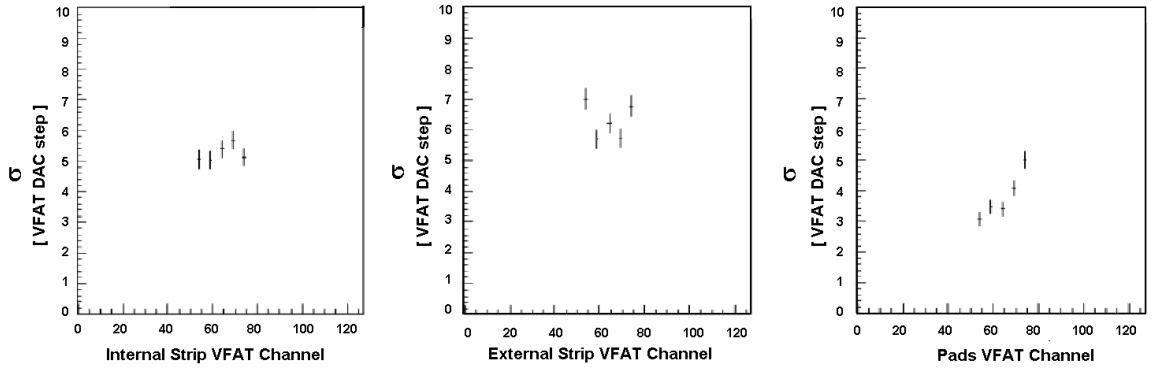

Figure 5.24: GEM read out by VFAT: noise σ of a group of internal strips with radii in the range 42.5 mm $\lesssim r \lesssim$ 93.3 mm (left), external strips with 93.7 mm $\lesssim r \lesssim$144.5 mm (middle), and a sector of pads (right), obtained with the calibration pulse scan available for the VFAT testing procedure. One VFAT DAC step corresponds to about 600 electrons.

dle plot) and pads (right-hand plot) obtained by varying the VFAT calibration pulse amplitude controlled by a Digital-to-Analog Converter (DAC), while keeping the threshold constant (see section 7.1, figure 7.6). An rms noise of $\sigma_{\text{noise}} \approx 5$ DAC units corresponds to about 3000 electrons. The pad noise clearly increases with the pad capacitance given in figure 5.25.

The CERN SPS beam test was important for understanding the response of the electronic readout chain to the typical signals of the GEM.

Events were triggered with two aligned scintillation counters of $5 \times 5\,\text{cm}^2$ size, positioned up- and downstream of the GEM chambers under test.

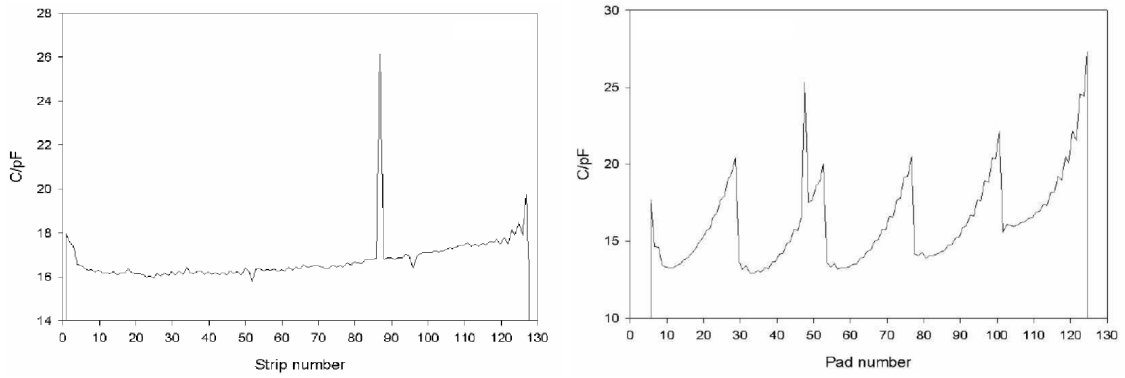

Figure 5.25: Capacitance measurement for strips (left) and pads (right). The spikes are caused by shorts between strips and pads.

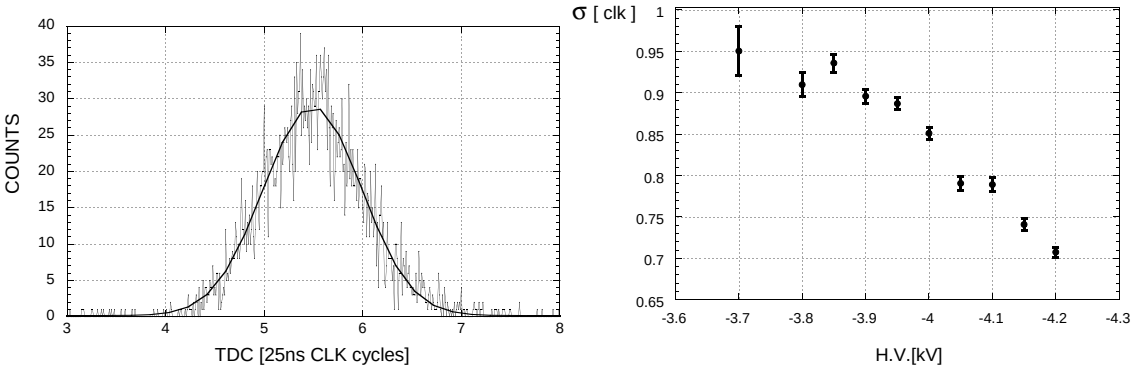

Figure 5.26: Left: distribution of the GEM VFAT trigger time with respect to the scintillator trigger time, measured with a TDC. Right: width σ, expressed in clock cycles, of the previous time distribution as a function of the high voltage.

Figure 5.26 (left) shows a measurement of the time difference between the GEM trigger signal and the scintillator trigger (asynchronous to the 25 ns clock), obtained with a TDC unit. The spread of this distribution, defining the time resolution of the GEMs, is shown in the right-hand plot as a function of the high voltage. As expected, increasing the voltage leads to a higher electric field and hence a shorter signal rise time with less time walk and a better time resolution.

The trigger time distribution extends over several clock cycles of 25 ns. Therefore, upon receiving a trigger, the readout has to accept signals within a time window covering several clock cycles, in order to avoid missing hits. The VFAT can accomplish this task by storing each hit in a programmable number of subsequent 25 ns bins of its memory (cf. section 7.1). An alternative approach for ensuring full efficiency is the reduction of the signal rise time by either increasing the electric field in the GEM or by adding CF_4 to the gas mixture.

Figure 5.27 shows the cluster size distribution for strips and pads at the typical HV of -4 kV. In figure 5.28 the mean cluster size is shown as a function of the high voltage and the VFAT threshold. The cluster sizes found are compatible with the results obtained by simulation.

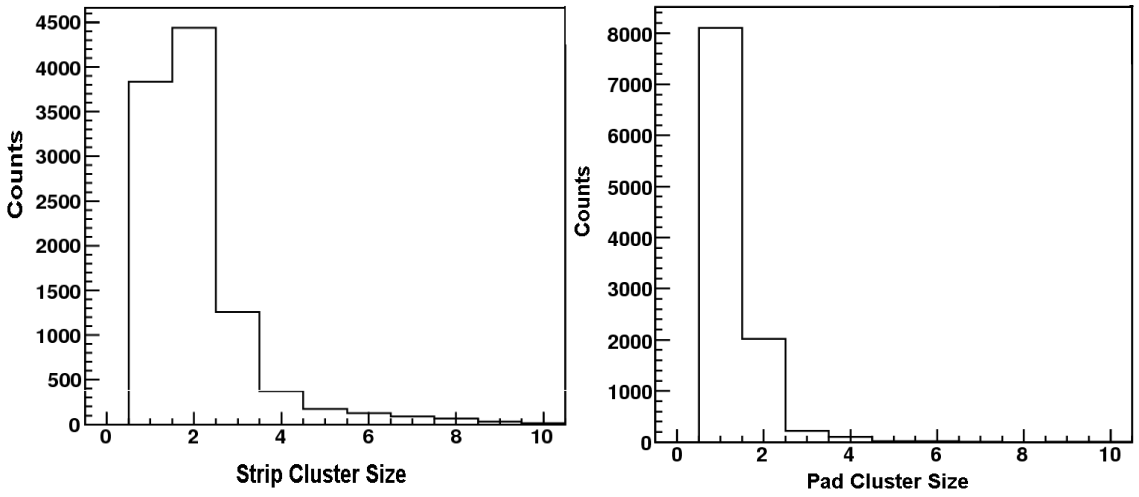

Figure 5.27: Strip and pad cluster size at HV $\approx -4.0\,\mathrm{kV}$, with a threshold of 40 DAC steps (or 24000 electrons) and a signal sampling time window of 2 clock cycles in the VFAT.

The cluster size distribution has an impact on the spatial resolution of the detector. For the operating parameters chosen for the tests underlying figure 5.27, pad clusters consist predominantly of only one pad, which leads to a resolution of $p/\sqrt{12}$ (where p is the pad width), ranging from $2\,\mathrm{mm}/\sqrt{12} \approx 580\,\mu\mathrm{m}$ to $7\,\mathrm{mm}/\sqrt{12} \approx 2\,\mathrm{mm}$. The strip clusters on the other hand contain mainly one or two strips, with approximately equal probability. Since tracks passing near the centre of a strip produce preferrably 1-strip clusters whereas tracks passing between two strips will rather give 2-strip clusters, the resolution will be better than for a pure 1-strip cluster population. While the precise value of the resolution depends on details of the charge sharing mechanism, one can expect it to lie in the range from $0.5\,d/\sqrt{12} \approx 58\,\mu\mathrm{m}$ to $d/\sqrt{12} \approx 115\,\mu\mathrm{m}$, where $d = 400\,\mu\mathrm{m}$ is the strip pitch. In the testbeam setup at hand, no external reference detector was available, which excludes a direct measurement of the resolution. However, with the hit measurements in two GEM planes and an approximate knowledge of the beam parallelism, a very rough consistency check is possible. Figure 5.29 shows the distribution of the radial distance between the strip cluster centres belonging to projective track hits in the two GEM planes with a distance $\Delta Z_{\mathrm{GEM}} = 395\,\mathrm{mm}$ along the beam. The observed standard deviation, $\sigma_{\mathrm{obs}} \approx 235\,\mu\mathrm{m}$, of this distribution can be decomposed according to the relationship

$$\sigma^2_{\mathrm{obs}} = 2\sigma^2_{\mathrm{GEM}} + \Delta Z^2_{\mathrm{GEM}}\sigma^2(\theta_{\mathrm{beam}})\,. \tag{5.1}$$

Solving (5.1) for the angular spread of the beam, $\sigma(\theta_{\mathrm{beam}})$, yields a value between 0.43 and 0.56 mrad which is well consistent with expectations for this beam.

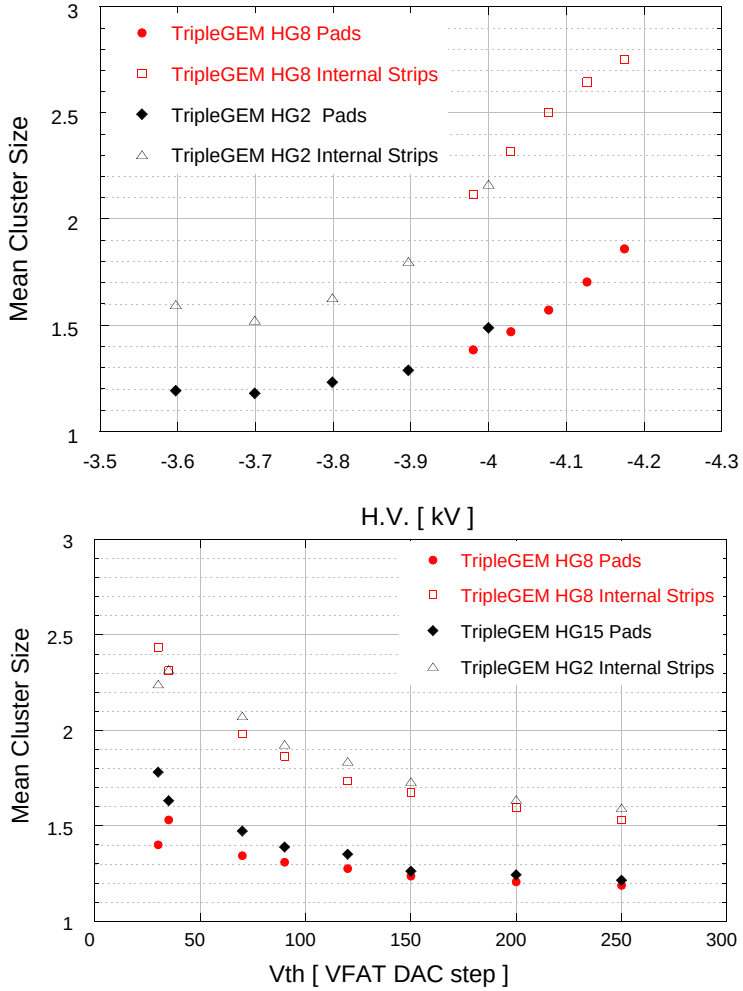

Figure 5.28: Cluster size for strips (open marker) and pads (filled marker) as a function of the high voltage for a threshold of 35 DAC steps (top), and as a function of the VFAT threshold for HV $= -4.1\,$kV (bottom) for different GEM planes (HG8, HG2, HG15). 1 DAC step corresponds to about 600 electrons. In all cases, the signal sampling time window in the VFAT was 2 clock cycles wide.

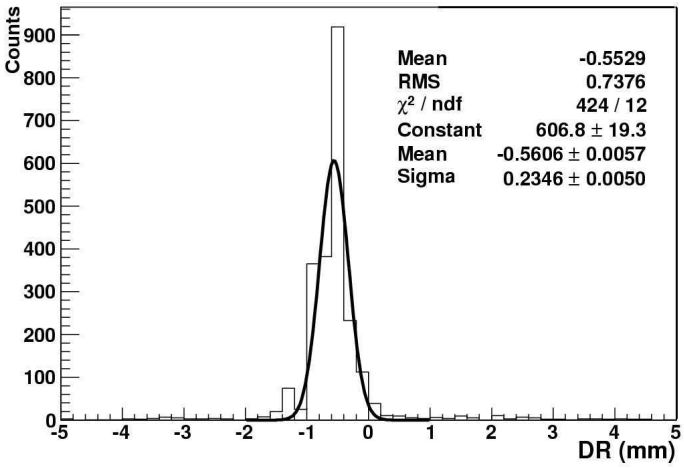

Figure 5.29: Radial distance of strip cluster centres belonging to aligned hits in two different T2 planes.